

Lei Chen

National Key Laboratory of Science and Technology on Helicopter Transmission, Nanjing University of Aeronautics and Astronautics, Nanjing 210016, China
e-mail: 742526683@qq.com

Guanghu Jin

National Key Laboratory of Science and Technology on Helicopter Transmission, Nanjing University of Aeronautics and Astronautics, Nanjing 210016, China
e-mail: meeghjin@nuaa.edu.cn

Qingwen Dai¹

National Key Laboratory of Science and Technology on Helicopter Transmission, Nanjing University of Aeronautics and Astronautics, Nanjing 210016, China
e-mail: daiqingwen@nuaa.edu.cn

Wei Huang

National Key Laboratory of Science and Technology on Helicopter Transmission, Nanjing University of Aeronautics and Astronautics, Nanjing 210016, China
e-mail: huangwei@nuaa.edu.cn

Xiaolei Wang

National Key Laboratory of Science and Technology on Helicopter Transmission, Nanjing University of Aeronautics and Astronautics, Nanjing 210016, China
e-mail: wxl@nuaa.edu.cn

Droplets Impacting and Migrating on Structured Surfaces With Imposed Thermal Gradients

In this work, the dynamic process of oil droplets impacting and migrating on structured surfaces with imposed thermal gradients was investigated. It was observed that on an isothermal smooth surface, a lubricant droplet would impact, spread to a maximum diameter, and retract; while on a non-isothermal smooth surface, an asymmetric geometrical morphology of droplet was generated, accompanying with a migration process. Relevant dimensionless parameters were employed to evaluate the dynamic process, and the physical mechanism was revealed. Decorating surfaces with convergent microgrooves pattern could not only increase the maximum spreading diameter but also accelerate the migration process. These are beneficial for the heat exchange efficiency and lubrication performances.
[DOI: 10.1115/1.4052779]

Keywords: Marangoni effect, droplet impact, thermocapillary migration, microgrooves, fluid film lubrication, interface

1 Introduction

The well-known Marangoni effect describes a liquid flow on a solid surface caused by liquid/gas interfacial tension gradient [1]. This phenomenon is referred to as thermocapillary motion when the solid surface experiences a temperature difference [2–5]. Over the past decades, investigations on the thermocapillary migration of liquid lubricants have been widely reported, including the fundamentals, the evaluations, and the manipulation strategies [6–9].

In real situations, liquid does not appear on a solid surface spontaneously, it either flows to the surface in the manner of liquid film or deposits on the surface in the manner of liquid mist. For instance, in aeroengine bearing chambers, liquid lubricants are dispersed into numerous droplets of different sizes due to high rotating speeds [10]. Once the droplets impact on the chamber wall, they wet the wall and form a lubricant film [11]. Bearing chambers always serve in a wide temperature range, and the formed liquid film could migrate from the warm to cold regions rapidly [12]. On the one hand, the impact and migration processes can take away the heat from bearing chamber, enhancing the heat exchange efficiency

[13]; on the other hand, liquid migration contributes to wet the rubbing surfaces [14]. The heat transfer and lubrication performances are two key indicators of aeroengine bearing chambers; it is of great importance to understand the impact and migration phenomena of liquid lubricants on non-isothermal surfaces.

Previously, water droplet impact on solid surfaces has been widely investigated, researchers have successfully fabricated microstructures patterns [15–18], superhydrophobic coating [19,20], or wettability gradient [21,22] to control water droplets impact dynamic. Since the surface tension and viscosity of commonly used lubricants is different from that of water, this discrepancy might yield a different impact phenomenon, especially when the surfaces are encountered with external thermal gradients, and besides, their potential applications are also different. Here comes some basic questions that what would happen to lubricant droplets when they collide on non-isothermal surfaces? Is there any inherent connection between the impact and migration processes? Examination of opening literatures indicates that investigations on these aspects are rarely reported.

Hence, we investigated the dynamic process of lubricant droplets on solid surfaces of different structures subjected to a thermal gradient. It was experimentally observed that lubricant droplets would impact, spread, and retract on isothermal smooth surfaces. An external thermal gradient could induce an asymmetric geometrical morphology of droplets, initiating the migration. Surfaces with different patterns of microgrooves were fabricated, and the dynamic features

¹Corresponding author.

Contributed by the Tribology Division of ASME for publication in the JOURNAL OF TRIBOLOGY. Manuscript received July 14, 2021; final manuscript received October 14, 2021; published online November 12, 2021. Assoc. Editor: Ramin Rahmani.

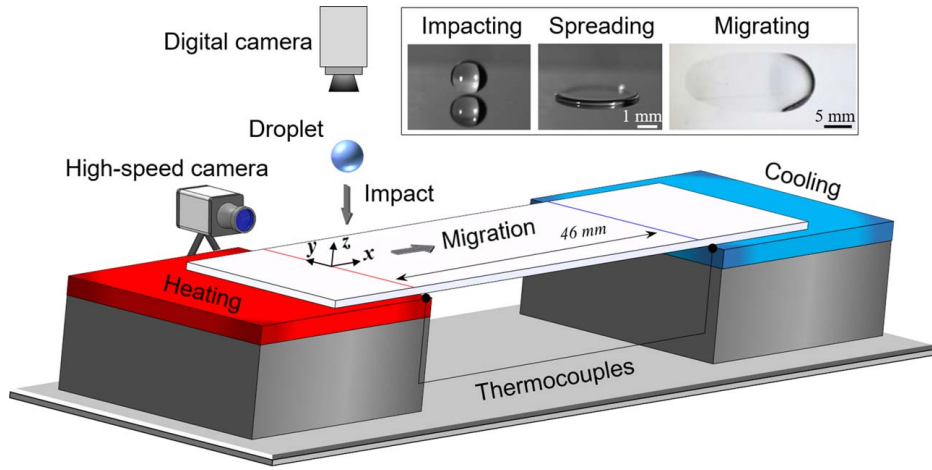


Fig. 1 Schematic of the experimental apparatus

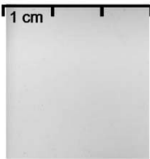
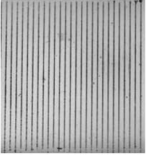
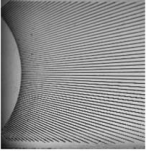
on these surfaces were discussed by quantifying the temporal variations in impact velocity, spreading diameter, thermal gradient, and migration distance. Relevant dimensionless parameters were employed to evaluate the dynamic processes, and the physical mechanism was revealed.

2 Materials and Methods

2.1 Materials. The solid specimens were made of SUS 316 stainless steel with dimensions of 75 mm × 30 mm × 3 mm, and all

testing surfaces were polished to an average surface roughness of ~50 nm. Microgrooves pattern were fabricated on the surfaces via lithography electrolytic etching technology, details about the process are available in Refs. [23,24]. Table 1 exhibits the photographic images and geometric parameters of the prepared patterns. Phenyl methyl siloxane (silicone oil) is widely used in rolling bearings due to its excellent characteristic of thermal stability. Here, a type of silicone oil with a viscosity of 100 mPa · s is employed for the tests (product number: D104762, Aladdin, China). Since the equilibrium contact angle of silicone oil on a smooth stainless

Table 1 Geometric parameters of the prepared microgrooves patterns

Groove orientation	Sketch map	Width (μm)	Initial pitch (μm)	Depth (μm)	Divergence angle (deg)
Smooth		<i>Na</i>			
Parallel		150 ± 10	800 ± 20	20 ± 4	<i>Na</i>
Perpendicular		150 ± 10	800 ± 20	20 ± 4	<i>Na</i>
Divergent		130 ± 10	200 ± 20	20 ± 4	3
Convergent		130 ± 10	200 ± 20	20 ± 4	3

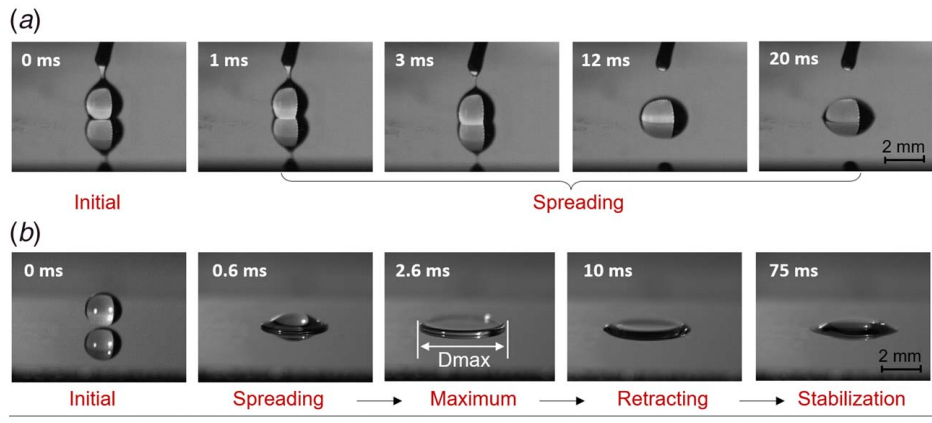


Fig. 2 Typical dynamic process of oil droplets on an isothermal smooth surface (a) without impact velocity and (b) with an impact velocity of 3.5 m/s

steel surface is ~ 13 deg, and silicone oil can totally spread into the microstructures (a typical wetting process is exhibited in Fig. S1 available in the Supplemental Materials on the ASME Digital Collection); thus, all prepared surfaces are regarded as mostly wetting state in this study.

2.2 Methods. Figure 1 shows the designed experimental setup to test the dynamic process. Two ends of the specimen are attached to temperature control components of a ceramic heater and a Peltier cooler, respectively. They are supported by Teflon blocks to reduce the heat losses. The available length for migration is ~ 46 mm. By setting their temperatures simultaneously, thermal gradients could be generated on the surface, which are measured by two type K thermocouples (accuracy of ± 2 °C).

Before experiments, the specimens were cleaned by ethanol and deionized water and blown dried with nitrogen, sequentially. Silicone oil droplets were placed at the same position via a micro syringe as the thermal gradient reached the set value. Via adjusting the needle diameter and its initial height, droplets with varying diameters and impact velocities were achieved. A high-speed camera (i-SPEED 726R, iX Cameras, UK) was employed to monitor the impact process, and the migration process was recorded by a digital camera (EOS 6D, Canon, Japan). The experimental conditions are shown in Table 2. For the thermal gradient of 2, 3.62, and 4.28 °C/mm, the temperature of the heater is 98, 173, and 206 °C, respectively; the corresponding temperature of the cooler is 6, 6.3, and 9.3 °C, respectively. The thermal gradients were chosen based on the relevant applications, in which the thermal gradient was between 0 and 10 °C/mm [25,26]. The insets clearly present the typical process of a silicone oil droplet on a smooth surface. Via extracting key frames from high speed and digital cameras, the spreading diameter and migration distance could be measured.

3 Results and Discussion

3.1 Droplets Impacting and Migrating on Smooth Surfaces. Figure 2 shows the dynamic process of silicone oil droplets ($d = 2$ mm) on an isothermal smooth solid surface. As shown in Fig. 2(a), when a droplet is gently placed on the solid surface (nearly

without impact velocity), it spreads to the surrounding slowly. As the impact velocity increases to 3.5 m/s (Fig. 2(b)), the droplet spreads to the surrounding rapidly and reaches the maximum spreading diameter (D_{max}) within 2.6 ms, after then, it retracts and remains stable on the surface. The results indicate that oil droplets impact on solid surfaces with a specific velocity would undergo a serial process of impacting, spreading, retracting and stabilization. This is different from water droplet dynamic under a similar impacting velocity, of which the droplet would experience prompt splash within spreading process and break-up within retracting process [27]. It is because that the viscosity of silicone oil is much larger than that of water, while the surface tension of silicone oil is much smaller. In this case, the viscous forces dominate the spreading and retraction process for silicone oil droplets, while water droplet dynamic is given by a competition between inertia and capillarity, resulting in different phenomena. Discussion on the dynamic process of silicone oil associated with the relevant nondimensional numbers will be presented in Sec. 3.3. Note that the contact angle was measured within ~ 5 s after the equilibrium state reached, which was much smaller than the apparent geometrical shape of the droplet within the initial impacting process shown in Fig. 2.

Figure 3 shows the impact and migration processes of silicone droplets on the isothermal ($\Delta T = 0$ °C/mm) and on-isothermal ($\Delta T = 3.62$ °C/mm) smooth surfaces. The initial diameter and impact velocity of droplets is 3 mm and 3.5 m/s, respectively. As shown in Fig. 3(a), whether the solid surface has a thermal gradient or not, liquid droplets would progress in the sequence of impacting, spreading, retracting, and stabilization. It is interesting to see that a thermal gradient can initiate a migration towards the cold side, resulting in an asymmetric geometrical shape of droplet [28]. Existence of temperature difference would yield a surface tension gradient between the warm and cold ends of the droplet; thus, liquid tends to flow to the cold side, stacking and forming an asymmetric geometry there.

Figure 3(b) shows the spreading diameter plotted as a function of time, note that a thermal gradient would contribute to a remarkable retracting process and yield a slightly larger maximum spreading diameter. This happens because the liquid viscosity decreases with increasing temperature; the viscous resistance force is smaller on the non-isothermal surface than that on the isothermal one, contributing to the liquid motion. Figure 3(c) shows the migration phenomenon occurs from the warm to cold sides, and the migration distance increases gradually as time elapsed, which is approximately 30 mm within 60 s. On the surface without thermal gradients, the migration distance is 0.

Confirming the impaction and migration phenomena of liquid droplets on solid surfaces with thermal gradients, key parameters of initial diameter, impact velocity, and thermal gradient on the dynamic process are investigated. Figure 4(a) shows the effect of initial diameter on the dynamic process under an experimental

Table 2 Experimental conditions at 25 °C

Initial diameter, d	2, 3 (± 0.1) mm
Droplet volume	5, 15 (± 0.5) μ L
Impact velocity, V	1.5, 2.5, 3.5 (± 0.1) m/s
Thermal gradient, ΔT	2, 3.62, 4.28 (± 0.02) °C/mm
Dynamic viscosity, μ	100 ± 5 mPa s
Surface tension, γ	20.8 ± 0.1 mN/m
Mass density, ρ	963 ± 5 kg/m ³

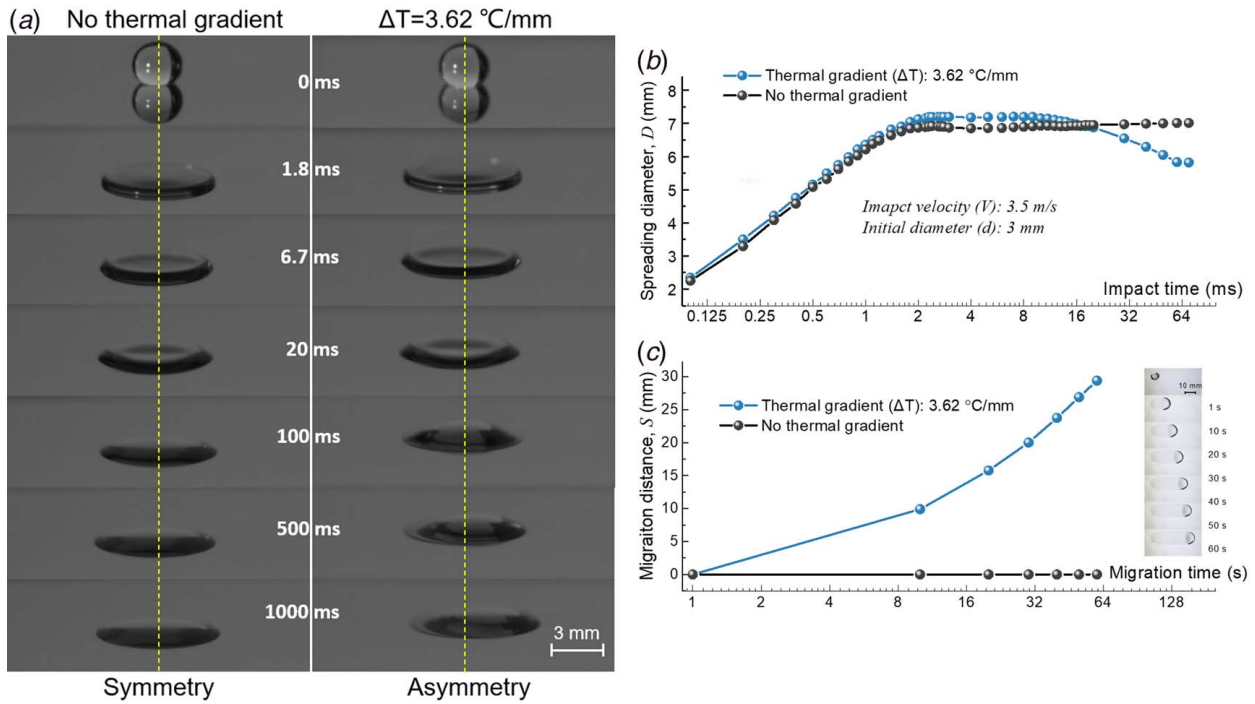


Fig. 3 (a) Symmetry/asymmetry impact phenomena on a smooth solid surface without/with a thermal gradient, (b) spreading diameter, and (c) migration distance versus the elapsed time

condition of $V = 3.5 \text{ m/s}$ and $\Delta T = 4.28 \text{ }^\circ\text{C/mm}$. For a droplet with an initial diameter (d) of 2 mm, the migration velocity and maximum spreading diameter is approximately 6.1 mm/s and 4.5 mm, respectively; when the d increases to 3 mm, the migration velocity and maximum spreading diameter increases to 7.3 mm/s and 7.2 mm, correspondingly. Figure 4(b) shows the effect of impact velocity on the dynamic process under an experimental condition of $\Delta T = 4.28 \text{ }^\circ\text{C/mm}$ and $d = 2 \text{ mm}$. As the impact velocity increases from 1.5 to 3.5 m/s, the maximum spreading diameter increases approximately 17.5%; while the impact velocity has a little effect on the migration velocity, which maintains at 6 mm/s under these three different impact velocities. Figure 4(c) shows the effect of thermal gradient on the dynamic process under an experimental condition of $d = 2 \text{ mm}$ and $V = 3.5 \text{ m/s}$. Note that a higher thermal gradient yields a larger migration velocity, and the migration velocity of $\Delta T = 4.28 \text{ }^\circ\text{C/mm}$ is 6.1 mm/s, which is nearly three times higher than that of $\Delta T = 2 \text{ }^\circ\text{C/mm}$.

Generally, a larger initial diameter or a faster impact velocity (a higher initial impact energy) could yield a higher amplitude of maximum spreading diameter, this trend is consistent with the

published investigations on water droplets [29]. Since the migration occurs accompanied by the impacting process, for a droplet with a larger maximum spreading diameter, the surface tension gradient between the warm and cold ends would be larger, which would yield a faster migration velocity. For the oil droplets under consideration, the heat conduction time scale (h^2/k) is of approximately 1 s, where h ($\sim 0.6 \text{ mm}$) is the droplet height and k ($\sim 0.15 \text{ mm}^2/\text{s}$) is the thermal diffusivity. The reason why the thermal gradient has a limited effect on the maximum spreading diameter is that the spreading process occurs within the initial 10 ms, this time scale is much smaller than the heat conduction time scale. However, after the droplet reached the maximum spreading diameter, the retraction process begins, and then thermal gradient plays a significant role, contributing to an asymmetric geometrical shape of droplet, as shown in Fig. 3(a). More details on the relationship between impact and migration will be presented in Sec. 3.3.

3.2 Droplets Dynamic on Structured Surfaces. Figure 5 shows the impact and migration processes of oil droplets on a

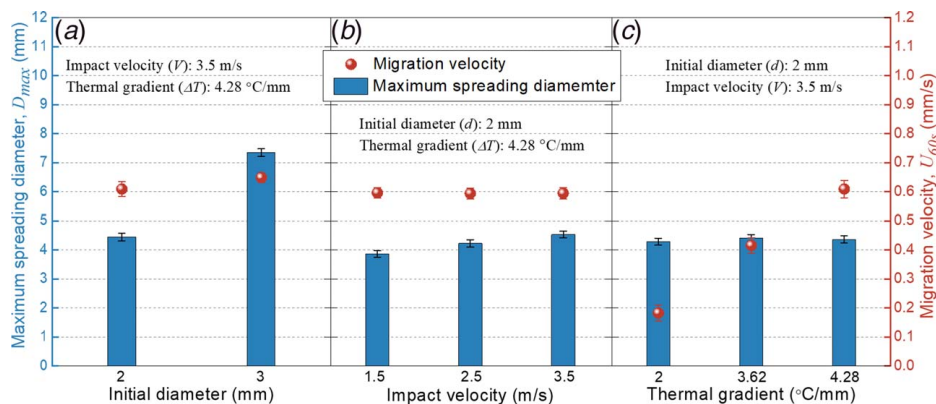


Fig. 4 Effects of (a) initial diameter, (b) impact velocity, and (c) thermal gradient on the maximum spreading diameter and the migration velocity on smooth surfaces

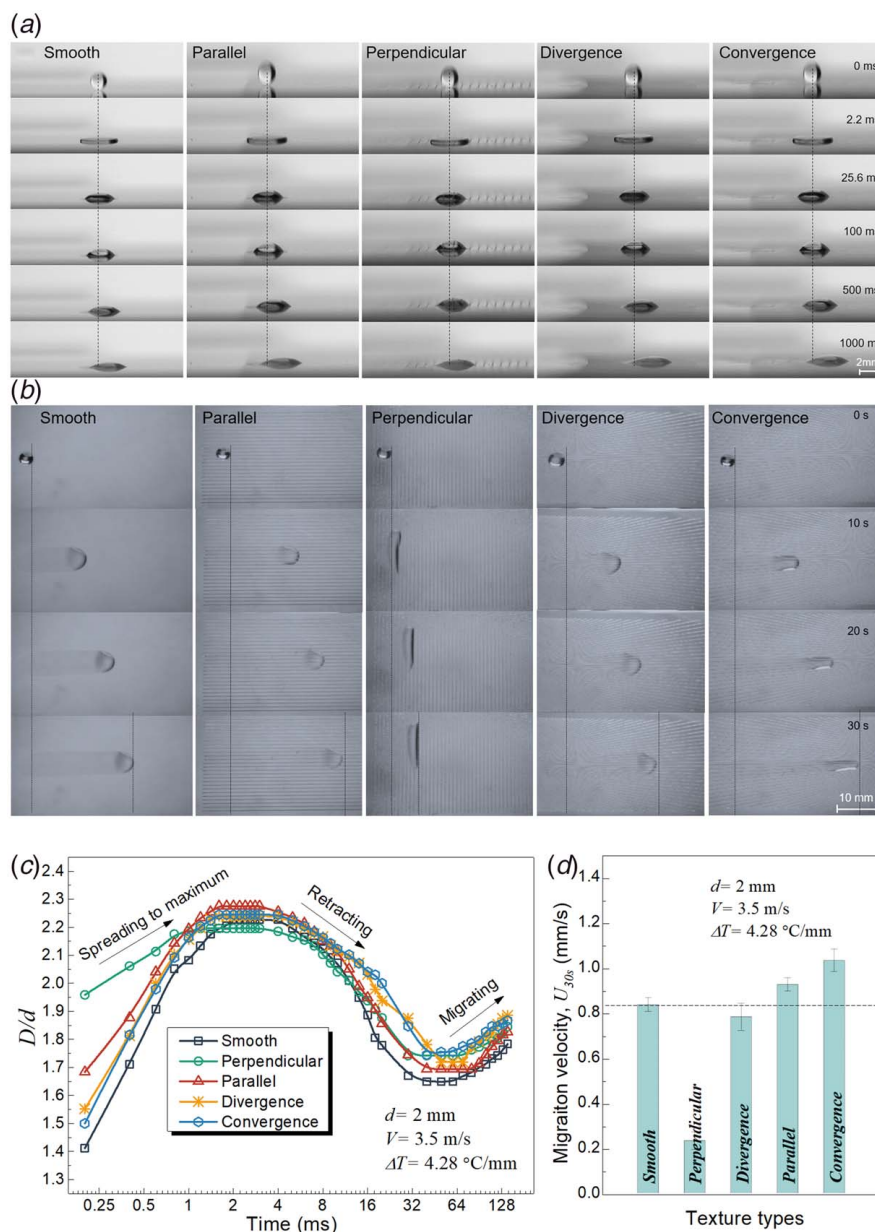


Fig. 5 Droplet dynamic on a smooth surface and surfaces with parallel, perpendicular, divergent, and convergent grooves under an experimental condition of $d = 2$ mm, $V = 3.5$ m/s, and $\Delta T = 4.28$ °C/mm: (a) impacting, spreading, retracting, and migrating process within the initial 1 s, (b) migration process within 30 s, (c) the dimensionless spreading diameter, and (d) the mean migration velocity versus the elapsed time

smooth surface and surfaces with parallel, perpendicular, divergent, and convergent grooves under an experimental condition of $d = 2$ mm, $V = 3.5$ m/s, and $\Delta T = 4.28$ °C/mm. As shown in Fig. 5(a), on surfaces with different microstructures, droplets would impact, spread, retract, and migrate to the cold side, sequentially. As the bottom panels of Fig. 5(a) exhibits (at 1000 ms), asymmetrical shapes of droplets are formed on these surfaces. Figure 5(c) shows the dimensionless spreading diameter with the elapsed time on these surfaces. Note that the diameters increase rapidly to maximum within ~ 4 ms, after then, droplets retract to minimum (at ~ 60 ms) and migrate to the cold side. Decorating surfaces with microstructures could affect the spreading diameter, and the surface with parallel grooves has a largest maximum spreading diameter.

The migration processes within 30 s are exhibited in Fig. 5(b), and the data are shown in Fig. 5(d). Obvious differences exist

among the migration velocities on these surfaces, which are in ascending order of perpendicular, divergent, smooth, parallel, and convergent. The velocity is ~ 1.03 mm/s on the surface with convergent grooves, while it is just ~ 0.23 mm/s on the surface with perpendicular ones. Overall, to achieve longer impact time, a surface with parallel grooves is suitable; while to achieve a faster migration velocity, a surface with convergent grooves is preferred.

3.3 Discussion

3.3.1 Droplet Impact. For the liquid droplets under consideration, its surface tension is small and viscosity is high (Table 2), the mean orders of magnitudes of Reynolds number ($Re = \rho V d / \mu$), Weber number ($We = \rho V^2 d / \gamma$), and Ohnesorge number ($Oh = \mu / \sqrt{\rho d \gamma}$) are ~ 10 , $\sim 10^2$, and ~ 1 , respectively (where ρ is the mass density, V is the impact velocity, d is the initial diameter,

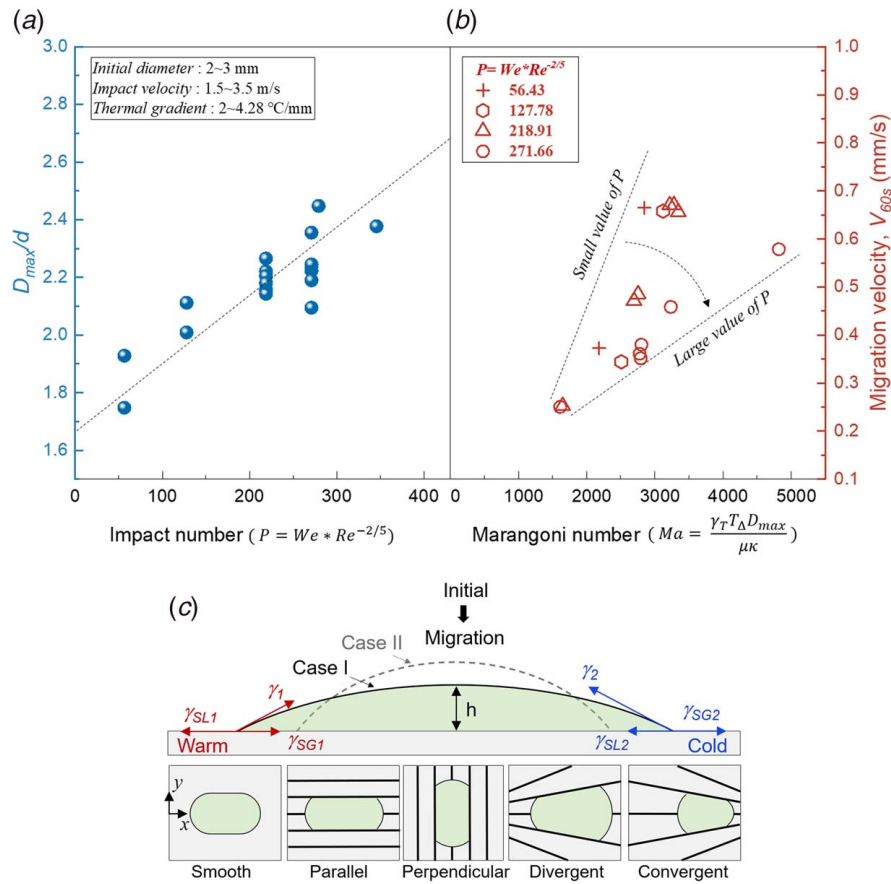


Fig. 6 (a) The relationship between the dimensionless maximum spreading diameter and the impact number, (b) the relationship between the migration velocity and the Marangoni number, and (c) ideal sketches of the droplets dynamic under different conditions

γ is the surface tension, and μ is the dynamic viscosity) [30]. Referring to these relevant numbers, it is believed that the inertia and viscous forces dominate the spreading process, while capillary and viscous forces dominate the retraction process [31]. Hereby, the dimensionless impact number ($P = We * Re^{-2/5}$) can be employed to quantify the impact dynamic [32].

3.3.2 Droplet Migration. Note that the surface tension of a liquid decreases with increasing temperature, a liquid would flow from low to high tension regions. When the oil droplet collides to a non-isothermal surface, the temperature difference generates a surface tension gradient along the free surface of droplet (Fig. 6(c), $\gamma_1 < \gamma_2$), inducing a migration from the warm to cold sides. The onset behavior of migration is determined by the ratio between the diffusive time scale ($\rho D_{max}^4 / \mu \kappa$) and the thermocapillary time scale ($\rho D_{max}^3 / T_{\Delta} \gamma_T$), where T_{Δ} is the thermal difference between the hot and cold sides ($T_{\Delta} \approx \Delta T \cdot D_{max}$), γ_T (~ 0.042 mN/m °C) is the surface tension coefficient, and κ (~ 1.56 mm²/s) is the thermal diffusivity [33]. Hereby, the relevant Marangoni number ($Ma = \gamma_T T_{\Delta} D_{max} / \mu \kappa$) is employed to quantify the migration dynamic.

The impact number (P) and the Marangoni number (Ma) are calculated and shown in Fig. 6. Note that the dimensionless maximum spreading diameter (D_{max}/d) is in a linear relationship with the impact number (P), and experimental data under different conditions all follow this trend. For the migration process, as shown in Fig. 6(b), under a specific impact number (P), the migration velocity (U_{60s}) increases gradually with increasing Marangoni number (Ma). This relationship can be adopted to predict droplet the impact and migration processes in real applications.

3.3.3 Relationship Between Impact and Migration. It is interesting to notice that there exists an internal relationship between the impact and migration processes. As shown in Fig. 6(b), when the impact number (P) is small, increasing the Marangoni number (Ma) would yield a rapid increasing in migration velocity. As the impact number (P) increases, the rate of increase of migration velocity with Marangoni number is reduced. This relationship can be explained as follows. The capillary and viscous forces dominate the retracting process, for a droplet with a larger D_{max} , more time is needed to retract. The longer the retracting time is, the later the migration will be. Mathematically, the theoretical migration velocity (U) can be simplified as [28,34]: $U \approx \Delta T \gamma_T h / 2 \mu$, where h denotes the droplet height. As sketched in Fig. 6(c), case I and case II represent a large and a small D_{max} , respectively. A larger impact number (P) would yield a larger D_{max} (Fig. 6(a)), forming a smaller h . Consequently, the migration velocity, and the rate of increase of migration velocity with Marangoni number, decreases with increasing impact number (P).

3.3.4 Droplet Dynamic on Structured Surfaces. As shown in Fig. 6(c), for a droplet impacting on a surface with parallel grooves, the grooves obstruct the spreading in the y direction and restrict the liquid between several grooves, which yields a small width in the y direction. While for the perpendicular ones, the spreading in the y direction is accelerated, generating a large width in the y direction. For the droplets under consideration, the maximum spreading diameter D_{max} is inversely proportional to width in the y direction, it means that the D_{max} is largest on the surface with parallel grooves and smallest on the surface with perpendicular ones. Similar phenomenon occurs on the surface with

divergent or convergent grooves, while the divergent or convergent gradient diminishes the influences of grooves; therefore, the corresponding D_{max} is between that of parallel and perpendicular ones. This is consistent with the experimental results in Figs. 5(a) and 5(c).

Note that the droplet height (h) is inversely proportional to its width in the y direction, thus, the h on the surface with parallel grooves would be higher than that on the smooth one, according to the above formula, the migration velocity would be faster. Besides, microgrooves act as micro capillaries, contributing to the migration [35]. Divergent grooves gradually contribute the spreading of liquid in the y direction, as time elapsed, the droplet height (h) decreases gradually, and the migration is weakened. While convergent grooves gradually limit the spreading of liquid in the y direction, and the droplet height (h) increases gradually, thus the migration is enhanced. For perpendicular grooves, it significantly obstructs the migration. Therefore, migration velocity on these surfaces is in descending order of convergent, parallel, smooth, divergent, and perpendicular (Fig. 5(d)).

3.3.5 Outlook. The droplet impact, droplet migration, relationship between impact and migration, and droplet dynamic on the structured surfaces were discussed. A qualitative comparison on the migration mechanism on surfaces with different patterns of microgrooves was provided. This discussion is benefit for understanding the migration mechanism. For a detailed comparison between theory and experiments one would need to resort to more detailed models, e.g., in the framework of CFD or a mathematical derivation.

Overall, understanding the impact and migration of oil droplets on a solid wall is relevant to many industrial applications such as printing, cooling of surfaces by sprays, and especially in tribo system with oil mist lubrication. The impact and migration processes of oil droplets affect the heat transfer and lubrication, and designing microgrooves on the chamber wall provides an effective manner to enhance the heat transfer and the lubrication performances.

4 Conclusions

In this study, experiments were designed to investigate oil droplets impacting and migrating on structured surfaces with imposed thermal gradients. It was observed that lubricant droplets would impact, spread, and retract on isothermal smooth surfaces. An external thermal gradient could induce an asymmetric geometrical morphology of droplets, initiating the migration. Dimensionless parameters of Weber, Reynolds, and Marangoni numbers were employed to evaluate the dynamic process, and the relationship between the impact and migration processes was revealed. Decorating surfaces with microgrooves pattern can control the dynamic process efficiently, of which convergent microgrooves pattern can not only increase the maximum spreading diameter, but also accelerate the migration process. These are beneficial for the heat exchange efficiency and lubrication performances of bearing chambers using oil mist for lubrication.

Acknowledgment

The authors thank the National Science and Technology Major Project (J2019-IV-0001-0068), the National Natural Science Foundation of China (Grant No. 51805252), and the Aeronautical Science Foundation of China (No. 2020Z040052002).

Conflict of Interest

There are no conflicts of interest.

Data Availability Statement

The datasets generated and supporting the findings of this article are obtainable from the corresponding author upon reasonable request. The authors attest that all data for this study are included in the paper.

References

- [1] Scriven, L. E., and Sterling, C. V., 1960, "The Marangoni Effects," *Nature*, **187**(4733), pp. 186–188.
- [2] Dai, Q. W., Khonsari, M. M., Shen, C., Huang, W., and Wang, X. L., 2016, "Thermocapillary Migration of Liquid Droplets Induced by a Unidirectional Thermal Gradient," *Langmuir*, **32**(30), pp. 7485–7492.
- [3] Bormashenko, E. Y., 2017, *Physics of Wetting: Phenomena and Applications of Fluids on Surfaces*, De Gruyter, Berlin, Germany.
- [4] Li, C., Zhao, D., Wen, J., and Lu, X., 2019, "Numerical Investigation of Wafer Drying Induced by the Thermal Marangoni Effect," *Int. J. Heat Mass Transfer*, **132**, pp. 689–698.
- [5] Dai, Q. W., Chen, S. Q., Huang, W., Wang, X. L., and Hardt, S., 2022, "On the Thermocapillary Migration Between Parallel Plates," *Int. J. Heat Mass Transfer*, **182**, p. 121962.
- [6] Grützmacher, P. G., Rosenkranz, A., and Gachot, C., 2016, "How to Guide Lubricants—Tailored Laser Surface Patterns on Stainless Steel," *Appl. Surf. Sci.*, **370**, pp. 59–66.
- [7] Grützmacher, P. G., Rosenkranz, A., Szurdak, A., Gachot, C., Hirt, G., and Mücklich, F., 2018, "Lubricant Migration on Stainless Steel Induced by bio-Inspired Multi-Scale Surface Patterns," *Mater. Des.*, **150**, pp. 55–63.
- [8] Yang, X., Zhuang, K., Lu, Y., and Wang, X., 2021, "Creation of Topological Ultrasmooth Surfaces for Droplet Motion Control," *ACS Nano*, **15**(2), pp. 2589–2599.
- [9] Dai, Q. W., Huang, W., Wang, X. L., and Khonsari, M. M., 2021, "Directional Interfacial Motion of Liquids: Fundamentals, Evaluations, and Manipulation Strategies," *Tribol. Int.*, **154**, p. 106749.
- [10] Flouros, M., Hendrick, P., Outirba, B., Cottier, F., and Proestler, S., 2015, "Thermal and Flow Phenomena Associated With the Behavior of Brush Seals in Aero Engine Bearing Chambers," *ASME J. Eng. Gas Turbines Power.*, **137**(9), p. 092503.
- [11] Sathyan, K., Hsu, H. Y., Lee, S. H., and Gopinath, K., 2011, "Development of a Centrifugal Oil Lubricator for Long-Term Lubrication of Spacecraft Attitude Control Systems—Design and Theory," *Tribol. Trans.*, **54**(5), pp. 770–778.
- [12] Liang, G., and Mudawar, I., 2017, "Review of Drop Impact on Heated Walls," *Int. J. Heat Mass Transfer*, **106**, pp. 103–126.
- [13] Höhn, B. R., Michaelis, K., and Otto, H. P., 2009, "Minimised Gear Lubrication by a Minimum oil/air Flow Rate," *Wear*, **266**(3), pp. 461–467.
- [14] Khonsari, M. M., and Booser, E. R., 2008, *Applied Tribology: Bearing Design and Lubrication*, John Wiley & Sons Ltd, Chi Chester.
- [15] Liu, Y., Andrew, M., Li, J., Yeomans, J. M., and Wang, Z., 2015, "Symmetry Breaking in Drop Bouncing on Curved Surfaces," *Nat. Commun.*, **6**(1), p. 10034.
- [16] Castrejón-Pita, J. R., Muñoz-Sánchez, B. N., Hutchings, I. M., and Castrejón-Pita, A. A., 2016, "Droplet Impact Onto Moving Liquids," *J. Fluid Mech.*, **809**, pp. 716–725.
- [17] Li, J., Hou, Y., Liu, Y., Hao, C., Li, M., Chaudhury, M. K., Yao, S., and Wang, Z., 2016, "Directional Transport of High-Temperature Janus Droplets Mediated by Structural Topography," *Nat. Phys.*, **12**(6), pp. 606–612.
- [18] Vaikuntanathan, V., and Sivakumar, D., 2016, "Maximum Spreading of Liquid Drops Impacting on Groove-Textured Surfaces: Effect of Surface Texture," *Langmuir*, **32**(10), pp. 2399–2409.
- [19] Liu, Y., Moevius, L., Xu, X., Qian, T., Yeomans, J. M., and Wang, Z., 2014, "Pancake Bouncing on Superhydrophobic Surfaces," *Nat. Phys.*, **10**(7), pp. 515–519.
- [20] Su, J., Legchenkova, I., Liu, C., Lu, C., Ma, G., Bormashenko, E., and Liu, Y., 2020, "Faceted and Circular Droplet Spreading on Hierarchical Superhydrophobic Surfaces," *Langmuir*, **36**(2), pp. 534–539.
- [21] Ma, Q., Wu, X., Li, T., and Chu, F., 2020, "Droplet Boiling on Heated Surfaces With Various Wettabilities," *Appl. Therm. Eng.*, **167**, p. 114703.
- [22] Lu, Y., Shen, Y., Tao, J., Wu, Z., Chen, H., Jia, Z., Xu, Y., and Xie, X., 2020, "Droplet Directional Movement on the Homogeneously Structured Superhydrophobic Surface With the Gradient Non-Wettability," *Langmuir*, **36**(4), pp. 880–888.
- [23] Yuan, S. H., Huang, W., and Wang, X. L., 2011, "Orientation Effects of Micro-Grooves on Sliding Surfaces," *Tribol. Int.*, **44**(9), pp. 1047–1054.
- [24] Dai, Q. W., Huang, W., and Wang, X. L., 2017, "Micro-Grooves Design to Modify the Thermo-Capillary Migration of Paraffin oil," *Meccanica*, **52**(1), pp. 171–181.
- [25] Roberts, E. W., and Todd, M. J., 1990, "Space and Vacuum Tribology," *Wear*, **136**(1), pp. 157–167.
- [26] Jones, W. R., and Jansen, M. J., 2008, "Tribology for Space Applications," *Proc. Inst. Mech. Eng., Part J*, **222**(8), pp. 997–1004.
- [27] Rioboo, R., Tropea, C., and Marengo, M., 2001, "Outcomes From a Drop Impact on Solid Surfaces," *Atomization Sprays*, **11**(2), pp. 155–165.
- [28] Wasan, D. T., Nikolov, A. D., and Brenner, H., 2001, "Droplets Speeding on Surfaces," *Science*, **291**(5504), pp. 605–606.
- [29] Thoroddsen, S. T., Etoh, T. G., and Takehara, K., 2008, "High-Speed Imaging of Drops and Bubbles," *Annu. Rev. Fluid Mech.*, **40**(1), pp. 257–285.

- [30] Roisman, I. V., and Tropea, C., 2002, "Impact of a Drop Onto a Wetted Wall: Description of Crown Formation and Propagation," *J. Fluid Mech.*, **472**, pp. 373–397.
- [31] Bartolo, D., Josserand, C., and Bonn, D., 2005, "Retraction Dynamics of Aqueous Drops upon Impact on non-Wetting Surfaces," *J. Fluid Mech.*, **545**, pp. 329–338.
- [32] Eggers, J., Fontelos, M. A., Josserand, C., and Zaleski, S., 2010, "Drop Dynamics After Impact on a Solid Wall: Theory and Simulations," *Phys. Fluids*, **22**(6), p. 062101.
- [33] Vanhook, S. J., Schatz, M. F., Swift, J. B., McCormick, W. D., and Swinney, H. L., 1997, "Long-wavelength Surface-Tension-Driven Benard Convection: Experiment and Theory," *J. Fluid Mech.*, **345**, pp. 45–78.
- [34] De Gennes, P., 1985, "Wetting: Statics and Dynamics," *Rev. Mod. Phys.*, **57**(3), pp. 827–863.
- [35] Fu, X., Ba, Y., and Sun, J., 2021, "Numerical Study of Thermocapillary Migration Behaviors of Droplets on a Grooved Surface With a Three-Dimensional Color-Gradient Lattice Boltzmann Model," *Phys. Fluids*, **33**(6), p. 062108.